BIOLOGY Methods & Protocols

Biology Methods and Protocols, 2020, 1–12

doi: 10.1093/biomethods/bpaa013
Advance Access Publication Date: 14 July 2020
Methods Manuscript

METHODS MANUSCRIPT

Pharmacophore-driven identification of N-methyl-D-receptor antagonists as potent neuroprotective agents validated using *in vivo* studies

Mukta Sharma [1,*], Anupama Mittal[1], Aarti Singh[1], Ashwin K. Jainarayanan[2], Swapnil Sharma[1], and Sarvesh Paliwal[1]

[1]Department of Pharmacy, Banasthali Vidyapith, Banasthali, Rajasthan, India and [2]Indian Institute of Science Education and Research, Mohali, Punjab, India

*Correspondence address. Department of Pharmacy, Banasthali Vidyapith, P.O. Banasthali, Rajasthan 304022, India. Tel: +91-1438-228341-348; E-mail: sharmamukta.924@gmail.com

Abstract

Alzheimer's disease (AD), apparently the most widespread reason behind dementia, is delineated by a continuous cognitive weakening in the aged. During its progression, N-methyl-D-aspartate receptor (NMDAR) antagonists are known to play a pivotal part in the mechanisms of learning and memory. Since there is an unmet medical need for the treatment of AD, we aim to identify possible chemical compounds targeted toward N-methyl-D-aspartate receptors. Three-dimensional models are developed to unveil some of the essential characteristics of the N-methyl-D-aspartate receptors by using a collection of already discovered N-methyl-D-aspartate receptor inhibitors. This is followed by virtual screening, which results in novel chemical compounds having the potential to inhibit N-methyl-D-aspartate receptors. Molecular docking studies and analysis promulgated two lead compounds with a high LibDock score. The compounds are shortlisted based on high estimated activity, fit values, LibDock score, no violation of Lipinski's, and availability for procuring. Finally, the shortlisted compounds are tested by employing *in vivo* studies, which we further propose as potential NMDA inhibitors for treating AD.

Keywords: Alzheimer's disease; N-methyl-D-aspartate; Discovery Studio; molecular docking

Introduction

Alzheimer's disease (AD) is a continuously developing neurological disorder represented by a decline in reasoning and thinking along with a tremendous neuronal impairment. The main characteristic features of this disorder include neurofibrillary tangles, amyloid plaques, and the degraded neurons in the incapacitated areas of the brain, for instance, the hippocampus. Although fundamental mechanisms of AD neuropathology are not well understood, upcoming pieces of evidence imply that altered NMDA receptor function and enhanced NMDA receptor-mediated excitotoxicity might add to both functional and pathological irregularity of AD. The N-Methyl-D-Aspartate receptor antagonists perform a central part in the mechanisms of learning and memory that are the most fundamental brain activities to be altered throughout the typical aging process [1]. The NMDA receptors are ligand-gated [2] ion channels in the central nervous system and are present presynaptically albeit at a high density postsynaptically [3, 4]. Recent literature evidence suggests that NMDA receptors exhibit tetrameric assemblies. Every subunit includes a large

Received: 21 March 2020; **Revised:** 25 June 2020. **Accepted:** 2 July 2020

extracellular amino-terminal domain [5]. In general, several localities covering the NMDA receptor can vigorously repress, initiate, or intensify its functioning. These NMDA receptors are attached to cation channels that are perforable to K+, Na+, and Ca2+ and high permeability to Ca2+ makes them suitable in mediating synaptic plasticity [6–8]. Furthermore, these features are essential and accountable for the development and various learning processes [9]. Literature evidence suggests that N,N′-diarylguanidine derivatives, the known NMDA receptor antagonists [10] possess essential characteristics such as high binding affinity and selectivity which makes them potential therapeutic chemical agents.

It is also a widely accepted fact that excessive NMDAR activity results in various neurological disorders, and many such inhibitors have not been successful in human clinical trials due to poor tolerance or are not as effective as expected. Therefore, in the present work, our goal is to identify novel and structurally diverse NMDA receptor antagonists through a well-defined sequential *in silico* virtual screening protocol followed by the biological evaluation of the lead compound. In this study, we compare our lead compound (HTS 00987) with a well-known drug "Memantine" which itself is an NMDA receptor antagonist that works by blocking increased levels of activity while saving normal activity. However, previous studies suggest that memantine has less efficacy in improving neuropsychiatric symptoms and it does not improve the functional ability of the patients. Moreover, a meta-analysis by Blanco *et al*. of memantine shows that its effect is indistinguishable from the placebo effect, which calls for an immediate search to find an alternate candidate with high efficacy for treating AD [11].

Here, the reported lead compound (HTS 00987), is, therefore, thoroughly validated by computational tools and tested by *in vivo* studies for the treatment of AD. We propose that this compound can further be subjected to clinical trials for its development as a novel drug to treat AD. To achieve that, we use a four-phase approach which includes ligand-based drug designing, structure-based virtual screening, molecular docking studies, and biological evaluation. In the first phase, we use the ligand-based drug designing methods, which utilize 3D properties of the ligands to estimate the biological activities. The selected pharmacophore model with a higher correlation value and a reasonable RMS fit are then subjected to pharmacophore mapping and various validation studies. In the second phase, we apply the validated models for the database search to retrieve the most potent compound. The lead compounds with good fit values, estimated activity, drug-likeness, and docking score are checked for novelty by employing pairwise Tanimoto similarity indices using "Find Similar Molecules by Fingerprint" in Discovery Studio (DS). In this study, all the lead compounds show low Tanimoto similarity indices to all the structures of known NMDA receptors antagonists validating their uniqueness [12]. The third phase entails molecular docking studies that succeeded by evaluating the retrieved potent lead compounds for neuroprotective activity. With the aim of combating AD, *in vivo* studies for the lead compounds are performed by using a radial arm maze model. Finally, by using a rigorous computational approach supported by experiments, we show that HTS 00987 exhibits a significant increase in the parameters like duration in the baited arm, reference/working memory error (WME), and percent age choice than memantine. We, therefore, propose HTS 00987 as a promising drug candidate that needs more detailed experiments for further assessment (see details in "Materials and methods" section).

Materials and methods

Pharmacophore modeling

Pharmacophore modeling is a robust and efficient approach for identifying a novel framework by using known ligands. Pharmacophore model was generated with an endeavor to represent the collection of key features that are vital for biological activity [13]. The HypoGen method was used for modeling pharmacophores [14]. This method utilizes the biological activities of the shortlisted chemical compounds to produce the system using DS V2.0 software. The "BEST" algorithm was employed to create conformers (~255) for every molecule together with an energy threshold of 20 kcal/mol [15].

Test and training set preparation

Generation of hypothesis entails sorting of chemical compounds in two different sets viz. training and test sets and requires specific rules. The chemical compounds selected in the training set should involve structurally diverse compounds (minimum 16) with co-occurring most active compounds. Preferentially, the activity range of this set must lie between three to five orders of magnitude. For this study, a set of 40 different chemical compounds was carefully chosen in the "training set" to produce the hypotheses. The biological activity values (IC50) of these compounds were in the range of 8–3000 nM. For the verification of the generated hypothesis, a test set was used in a related manner to the training set that included 19 chemical compounds with reasonable structural variance and biological activities [16]. Chem Draw 8.0 was used for illustrating the structures of all compounds. As previously mentioned, the "BEST" algorithm was applied to produce energy-minimized conformers (a maximum of 255) for every molecule including an energy threshold of 20 kcal/mol. These conformations were used for hypothesis generation using DS [17, 18].

Pharmacophore generation using HypoGen

A 3D pharmacophore model was generated after assessing the biological activities of chemical compounds present in the training set. Vital chemical features were selected for producing the hypothesis by applying "feature mapping module" of DS [19]. During the hypotheses generation, hydrogen bond donor (HBD) and hydrophobic (HY) were chosen depending on the compounds present in the training set [20]. The pharmacophore models were predicted by implementing the "3D QSAR Pharmacophore module" of DS and hypotheses with reasonable scores were picked for additional validation [21, 22]. The hypotheses with the highest scores were shortlisted on the basis of correlation, RMS, weight, configuration, cost values viz. fixed, null, and total [23, 24].

Assessment of pharmacophore quality and database screening

The quality of shortlisted pharmacophore models was estimated by using three distinct approaches. Primarily, the data were rearranged for validation using Fischer's randomization test. The findings confirmed that the hypotheses produced are reasonable [23, 25]. A correlation value of 0.65 was observed amidst the experimental and predicted activities of the test set compounds. Finally, an external test set was used along with a well-known marketed drug namely memantine for the validation [26].

Methods for validating pharmacophores:

Fisher's cross-validation test

Fisher's randomization test was employed to estimate the statistical significance of the models generated by using the training set. The datasets generated by Fischer's randomized tests yield pharmacophoric models and reasonable values of cost, RMS, and correlation of the models recommend remodeling of the pharmacophores. With the help of the cat scramble program (available in the Catalyst HypoGen module), the biological activities of the chemical compounds in the training set were reviewed and employed for generating hypotheses. Therefore, every parameter was used in a similar fashion to the initial HypoGen calculation. It was observed that, at a 99% confidence level, cat scramble created 99 spreadsheets [27, 28].

The internal test set validation

The generated model was validated by employing a test set comprising 19 distinct chemical compounds. The estimated value of the test set compounds was assessed by considering the r^2 values (squared correlation coefficient). The estimated activities were calculated by mapping molecules in the test set over the pharmacophore model and assessing their corresponding fit values. The fit value depends on the number of pharmacophore features that superimpose on to the relevant chemical groups. Furthermore, the compound with full feature mapping was compared with others in the dataset [29, 30].

An external test set validation

For rigorous validation of the pharmacophore, an external dataset of NMDAR inhibitors was used with the actual activity ranging from 8 to 3000 nM. The compounds in this dataset were mapped over the derived pharmacophore model. It was also validated by mapping a well-known marketed drug "memantine" which is an NMDAR-based inhibitor as an additional quality check method. The fit values and the range of the estimated and actual activities of the dataset were thoroughly examined [31].

Virtual screening

Virtual screening, a broadly used tool for identification of leads *in silico* has helped the pharmaceutical industry to increase the chances of designing medicines in lesser time [32]. Though a thoroughly examined pharmacophore model contains vital chemical features accountable for biological activities of potential drugs, it can be used as an input for a database search. As mentioned before, the hypothesis with the considerable score was utilized as an input for obtaining effective molecules from the databases such as National Cancer Institute (NCI) and Maybridge [33]. The "best conformer generation method" was used for retrieving the conformers of every molecule with an energy threshold of 20 kcal/mol. To begin with, the compounds were sorted based on Lipinski's "Rule of five" that introduces the foundations for drug-like properties [34]. Lipinski's rule of five suggests that "a compound is suitable for further studies only if Molecular weight $>$ 500, log $P > 5$, hydrogen bond donors $>$ 5, and hydrogen bond acceptors $>$ 10". Furthermore, the molecules which showed a complete feature mapping over the query pharmacophore model was selected as a hit [35]. The selected pharmacophore model was used as an input for the databases to retrieve the compounds that mapped over all the chemical features of the selected pharmacophore. Compounds were further sorted based on higher fit values and full feature mapping. A higher fit value indicates good matches. The compounds qualifying all these requirements were further shortlisted for carrying out molecular docking studies [36].

Molecular docking studies

To understand the nature of molecular interactions of the lead compounds, we carried out molecular docking studies using DS [37, 38]. LibDocker, a molecular dynamics annealing-based algorithm, which is accessible as an extension of DS V.2.0, was used for the docking studies [39, 40]. The crystal structures to be used for docking studies were obtained from PDB. The receptor protein was assessed for the missing valencies, hydrogens, and was checked for any structural refinement if needed. The selected protein was divided into two segments: the protein and the ligand. The protein segment was designated as a receptor molecule while the ligand was used to describe the binding site of approximately nine angstroms on the receptor molecule. The chemical structure of the test compound was sketched and subjected to energy minimization to get the highly stable structure for molecular docking studies [37, 41, 42]. Based on present coordinates, marketed drug and test compounds were employed to molecular docking studies. The analysis was run by retaining the parameters to their preselected values. In the end, all possible interaction modes were analyzed based on LibDock scores.

Biological evaluation

With no known treatment for AD to date, it has become one of the biggest challenges in the field of medicine. Based on high estimated activities, fit values, LibDock score, the violation to Lipinski's, and availability for procuring, one compound (HTS 00987) was finally subjected to *in vivo* studies on mice using an eight-arm radial maze [43, 44]. This study was carried out into two distinct cliques to measure the impact of extended therapy of diazepam-effected amnesia [45, 46]. All experimental studies were conducted in the animal laboratory at the Department of Pharmacy, Banasthali University. The mice were grouped and caged in plastic cages with regular water and diet for rodents. We administered test drug to the mice in the first and second cliques for 7 and 14 days, respectively. All experiments performed were approved by the Institutional animal ethical committee of the Banasthali University. Young albino healthy male mice with 15–20 weeks of age, weighing 25–30 g, provided by the Chaudhary Charan Singh Haryana Agricultural University - Hisar were used for behavioral testing. This study was performed according to the OECD 432 guidelines. A group of 36 mice was split into two cliques of three groups (control, standard and test group) separately. The animals of clique I and II were treated for 7 and 14 days, respectively. Mice were delivered two trials: (i) one in the morning through 9:00 a.m. and (ii) one in the evening through 6:00 p.m. Every trial started with the careful cleaning of the maze by using 70% ethanol. Two arms (no. 1 and no. 3) of the arm maize were baited with food. Mice were carefully placed in the middle of the octagon and were granted a free choice. All the movements were recorded to analyze the correct selection of baited arm later. The arms of the maze were not rebaited, therefore, the earliest admission inside the baited arm was recorded as the correct choice [47, 48]. After 3 weeks of training, the control group of mice was given carboxymethylcellulose (CMC 0.5%), standard group was administered with memantine (5 mg/kg), and test group was given HTS

00987 (5 mg/kg) twice (10:00 a.m. and 7:00 p.m.) at the same time on each day orally for a period of 7 and 14 days. The experimental study was designed such that we were able to assess the impact of CMC, memantine, and HTS 00987 after the completion of the treatment (Days 7 and 14) against diazepam-effected amnesia [49–51]. After the completion of 7 and 14 days, (which marked the end of treatment), we administered diazepam to all the animals (1 mg/kg i.p.) 60 min later the drug administration (test drug). Since the first group of every clique toiled as a control, we excluded this group for diazepam administration. The cognitive parameters were assessed 30 min later the administration of the inducing agent (diazepam) using an eight-arm radial maze, which corresponds to learning [52]. The lead compound HTS 00987 was evaluated for behavioral studies using diazepam-induced amnesia in mice model. The mice were allowed to be at the center of the octagon of radial arm maze on the Days 8 and 15, respectively [53]. To investigate the effect of control/CMC, memantine, and HTS 00987 on Wistar albino mice, five parameters were examined: the number of entries in the baited arm, duration in the baited arm, percent correct choice, reference memory error (RME), and WME using Orchids *ALL MAZE* software version 4.0 (Orchid Scientific, Maharashtra, India) [54–56]. Percent choice was estimated by halving the correct number of entries by the complete number of entries in the baited arm and multiplied by 100. Entrance in an unbaited arm was counted as a RME, and re-entrance to the baited arm was marked as a WME [57]. Average values for all parameters were determined for Week 1 (1–7 days) and Week 2 (8–14 days) and one-way ANOVA was computed for whole data.

Results and discussion

HypoGen model for N,N′-diarylguanidine inhibitors

In this study, we collected a set of 40 diverse compounds with their corresponding biological activities from the literature. The training set with extensive diversity includes the N,N′-diarylguanidine inhibitors of NMDAR antagonists. Biological activities and chemical structures of all the presynthesized chemical compounds are presented in Table 1. A 3D QSAR pharmacophore generation module of the DS is used to produce pharmacophore model by utilizing different chemical features such as hydrogen bond acceptor, HBD, HY, ring aromatic, and positive ionizable [23]). On the basis of activity values of the training set molecules, 10 top-scored hypotheses are produced. The best 10 hypotheses are comprised of only two features: HBD and HY. Hypo1 contains two HBD and three HY, which highlight the biggest cost difference (69.23), best correlation coefficient (0.91), highest fit value (9.296), and lowest root mean square deviation (RMSD) of 0.88. The fixed and the null cost values are found to be 146.091 and 231.594, respectively, where "fixed total cost" is dependent on the sum of the cost components including weight cost, error cost, and configuration cost. Principally, there are two essential contents that are practiced for cost analysis: (i) the difference between null and total cost (cost difference) and (ii) the difference between the fixed and null costs. The "fixed cost" corresponds to a cost of the general hypothesis, which ultimately predicts the strength of chemical compounds in the training set with the least divergence. However, the "null cost" signifies the cost of a hypothesis. The difference between these two costs should be greater than "70 bits" for explaining the statistical significance of the model. The cost difference must be larger than "60 bits" to imply actual data. The results presented here have revealed that all the hypotheses have the HBD and HY group, implying that chemical features: HBD and HY impersonate a vital role in N,N′-diarylguanidine inhibition. We observe that the cost difference within the "null and fixed cost" is 85.50, which is clearly >70 bits. Every generated hypothesis exhibits a correlation coefficient >0.79, however, the top-scoring hypothesis (Hypo1) displays the greatest correlation coefficient value of 0.91, confirming the real prognostic ability of the top-scoring hypothesis (Hypo1). It also exhibited a high-cost difference and correlation value with lower RMSD values as compared to the remaining hypotheses.

Thus, the top-scoring hypothesis (Hypo1) is considered as the "soundest hypothesis" and employed to other analysis. Figure 1 displays the chemical features of "Hypo1". In an attempt to test the prognostic precision of "Hypo1", the compounds in the training set are employed and regression analysis is carried out to estimate the activities of every compound in the training set. It is observed that "Hypo1" is proficient to assess the activities of compounds. The experimental and estimated activities for compounds in the training set are presented in Table 2. A graph plotted between the observed activity and estimated activity exhibits a substantial correlation coefficient ($r^2 = 0.83$) for training set compounds, indicating a high predictive ability of the pharmacophore as shown in Fig. 2.

Validation of hypothesis

Validating the hypothesis for further studies is a vital step in drug development. There are several known methods such as (i) selecting chemical compounds for validating pharmacophore model and its features, (ii) Fischer's randomization method, and (iii) an external set of compounds that can assess the quality of pharmacophore. These methods are explained below.

Fischer randomization method

The foremost reason for this assessment is to confirm the robust correlation amid the structures and biological activities of compounds [58]. The Fischer's validation method is implemented at a confidence level of 99% to the generated HypoGen model, where 99 random hypotheses were produced (Fig. 3). Various pharmacophore hypotheses are generated by randomly creating the hypotheses and matching the activity data of the compounds in the training set with the characteristic features and criterion used for producing the new hypothesis. We observe that all the hypotheses exhibited a higher cost score than the primary hypothesis thus supporting that the top-scoring hypothesis was not obtained randomly. This validation suggests that hypotheses generated using this method did not show activity values comparable to that of the top-scoring hypotheses (Hypo1) as shown in Fig. 3. On analyzing the 99 runs, the value of correlation coefficients is found to be relatively low as shown in Fig. 4. Additionally, the RMS values and other important values such as total costs and the null cost are found to be elevated. Hence, this procedure assured the credibility of the chosen pharmacophore model (Hypo1).

Internal test set validation

In order to strengthen the validity of the generated hypothesis, a set of 19 chemical compounds was selected for additional confirmation. The selected chemical compounds are employed to pharmacophore feature mapping. Figure 5 represents a plot between actual and estimated activities of the test set with $r^2 = 0.65$. This simply confirms the authenticity of the selected pharmacophore model.

Table 1: Structures and biological activity of N,N′-diarylguanidine derivatives as NMDA receptor antagonists

N,N′-diarylguanidine derivatives

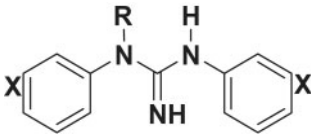

Name	X	R	IC_{50} nM (SEM)*
5	2-CH_3	H	31 (±3)
6	H	H	397 (±21)
7	2-C_2H_5	H	14 (±1)
8	2-$CH(CH_3)_2$	H	88 (13)
9	2-$C(CH_3)_3$	H	356 (±63)
10	2-I	H	13 (±1)
11	2-OCH_3	H	1990 (±270)
12	2-C_6H_5	H	8110 (±40)
13	3-CH_3	H	43 (±5)
14	3-C_2H_5	H	8 (±2)
15	3-$CH(CH_3)_2$	H	96 (±18)
16	3-$(CH_2)_2CH_3$	H	42 (±4)
17	3-I	H	125 (±1)
18	3-OCH_3	H	351 (±39)
19	4-CH_3	H	535 (62)
20	4-C_2H_5	H	245 (±38)
21	4-$CH(CH_3)_2$	H	242 (±27)
22	4-Br	H	33 (±3)
23	2-CH_3	CH_3	6280 (360)
24	3-CH_3	CH_3	247 (±17)
25	3-C_2H_5	CH_3	82 (±10)

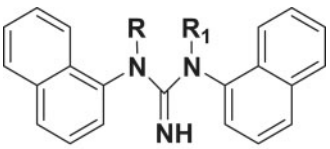

Name	**R**	**R_1**	**IC_{50} nM (SEM)**
26	H	H	165 (±28)
27	H	CH_3	4800 (±130)
28	H	C_2H_5	6130 (470)
29	H	C_6H_5	7930 (±1490)
30	CH_3	CH_3	10 700 (±1400)
31	CH_3	C_2H_5	8480 (±890)
32	CH_3	C_6H_5	11 000 (±700)
33	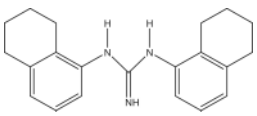		59 (±3)
34	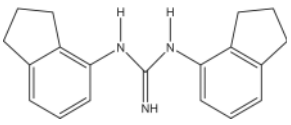		29 (±8)
35	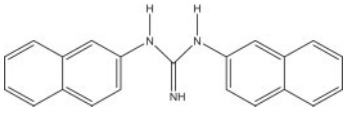		92 (±9)

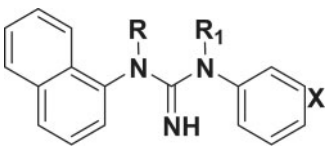

Table 1: . (continued)

N,N′-diarylguanidine derivatives

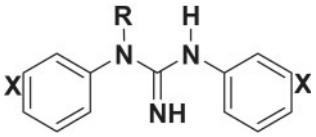

Name	X	R	IC_{50} nM (SEM)*

Name	**X**	**R**	**R_1**	**IC_{50} nM (SEM)**
36	3-C_2H_5	H	H	54 (±5)
37	2-$CH(CH_3)_2$	H	H	91 (±9)
38	2-I	H	H	40 (±7)
39	3-CH_3	H	H	75 (12)
40	3-C_2H_5	H	CH_3	2540 (±670)
41	3-C_2H_5	H	C_2H_5	2190 (±360)
42	3-C_2H_5	CH_3	H	1000 (±60)
43	2-$CH(CH_3)_2$	CH_3	H	7250 (±640)
44	3-CH_3	H	CH_3	1860 (±180)
45	3-NO_2	H	CH_3	6260 (±700)
46	3-NH_2	H	CH_3	2700
47	3-N_3	H	CH_3	3020 (±20)
48	3-NO_2	CH_3	H	2640 (±370)
49	3-NH_2	CH_3	H	13 000 (±300)
50	3-N_3	CH_3	H	2740 (±220)
51	H	H	CH_3	2900
52	3-C_2H_5	CH_3	CH_3	1210 (±60)
53	3-C_2H_5	C_2H_5	CH_3	2290 (±160)

Name	**Structure**	**IC_{50} nM (SEM)**
54		1370 (40)
55	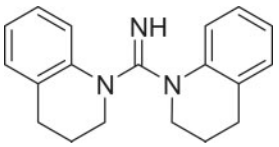	7180 (±310)
56	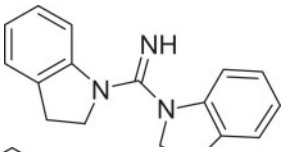	341 (73)
57	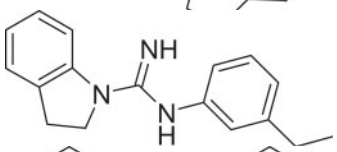	1070 (±260)
58	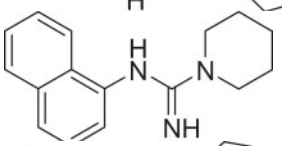	1410 (±100)
59	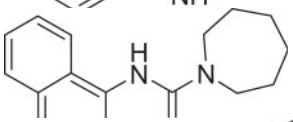	343 (±32)
60	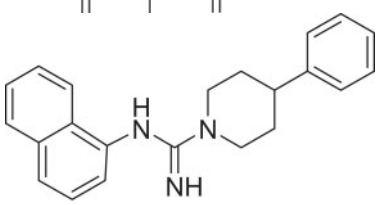	60 (±8)
61		240 (15)
62		2100 (160)
63		140 (13)

*IC_{50} values are mean ± standard error of measurement (SEM) and are the results of a minimum two determinations. No SEM indicates a single determination.

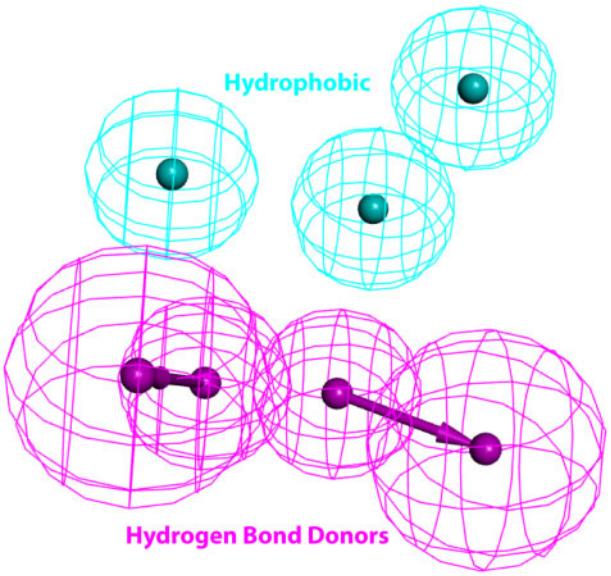

Figure 1: Pharmacophoric features identified from best hypothesis 1.

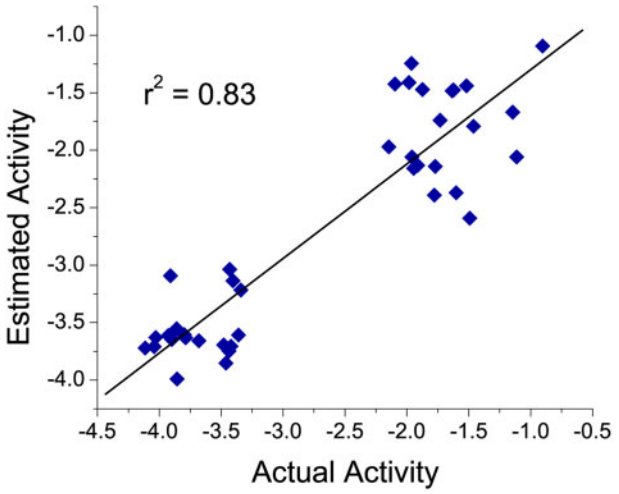

Figure 2: A plot of actual versus estimated biological activity for training set compounds.

Table 2: Results of the top 10 pharmacophore hypotheses generated by the HypoGen algorithm

Hypotheses	Total cost	Cost difference	RMSD	Correlation	Feature
1	162.357	69.24	0.888	0.91	2HBD, 3HY
2	172.697	58.90	1.16	0.85	2HBD, 2HY
3	173.557	58.04	1.23	0.84	2HBD, 2HY
4	177.246	54.35	1.31	0.82	2HBD, 3HY
5	181.839	49.75	1.32	0.80	2HBD, 2HY
6	182.56	49.03	1.35	0.79	2HBD, 3HY
7	182.96	48.63	1.394	0.78	2HBD, 2HY
8	186.94	44.65	1.414	0.78	2HBD, 3HY
9	186.98	44.61	1.382	0.77	2HBD, 3HY
10	185.03	43.24	1.341	0.76	2HBD, 3HY

External test set validation

The major aim of generating pharmacophore models is their use for identifying and optimizing leads/hits that leads to the paradigm of drug discovery and development. However, for further studies, there is a need to assess the characteristics of the generated model(s). To validate the model, a set of chemical compounds is used to evaluate the features of the generated model. Here, we validate the generated pharmacophore by employing an external set of structurally diverse NMDAR inhibitors with an actual activity ranging between 0.068 and 2.1 nM. The compounds in this set are later subjected to pharmacophore mapping. All the important parameters such as fit values and the variation in the estimated and actual activities of all the compounds are reviewed extensively. The pharmacophore feature mapping of the best-fit molecule in the external test set is shown in Fig. 6. The predicted and the actual activity for external test set compounds (Fig. 7 with $r^2 = 0.87$) testifies the universality of the Hypo1.

Database screening

Thoroughly verified top-scoring hypothesis (Hypo1) is employed as an input for obtaining appropriate chemical compounds from biochemical databases such as NCI (238 819 compounds) and Maybridge (59 652 compounds). Consequently, the first screening resulted in 171 and 299 compounds from NCI and Maybridge, respectively [58]. The obtained chemical compounds are refined based on Lipinski's violation and the calculated activity values calculated by top-scoring hypothesis (Hypo1). Ten potential compounds are selected after refining a total of 470 hits which display a complete feature mapping with a considerable fit value varying from 10.18 to 7.775, respectively, and zero Lipinski's violation as shown in Table 3.

Molecular docking studies

Molecular docking is a robust computative method that marks the possible conformations of chemical compounds in the binding sites of the protein. The hallmark to determine the quality of this method is preciseness that identifies the accurate binding modes of the ligand to the targeted protein. The center of the active site of N-methyl-D-aspartate receptor antagonists comprised Tyr214, Thr174, Ser173, Thr116, Arg121, Ser114, Gly172, and His88 which are the significant residues surrounded in this region. Ten (five Maybridge and five NCI) hits acquired from the databases satisfying drug-like properties, as well as one marketed drug (memantine), are docked in the binding site of 3OEK (using LibDock module executed in DS). A number of 300 different confirmations (otherwise known as poses) are produced for every compound. Of these 300, first 10 confirmations (poses) are assessed for every molecule by examining their LibDock score ranging between 95.214 and 114.714. We notice that HTS 00987 (Maybridge) exhibits a high LibDock score of 114.714 whereas memantine (marketed drug) shows the score of 70.16.

The interaction analysis of HTS 00987 reveals that hydrogen present on second and fifth positions of benzodioxol ring is involved in Van der Waals interactions with Tyr214 and Thr174. Amine and hydrogen present on 1-ethylamino-3-methoxy-2-methylpropan-2-ol show hydrogen bond and Van der Waals interactions with Pro170, His88, and Lys87, respectively, as shown in Fig. 8A. Interaction analysis of reference drug memantine reveals that the amine group present on the adamantan-1-amine ring is involved in hydrogen bond interactions with Ser131, Tyr282, Gly264, and Ser260. Methyl present on the third and fifth position of amine ring showed Van der Waals interactions with Asp283, His127, and Arg292 as shown in Fig. 8B. Another carbon present at the second and third positions of the

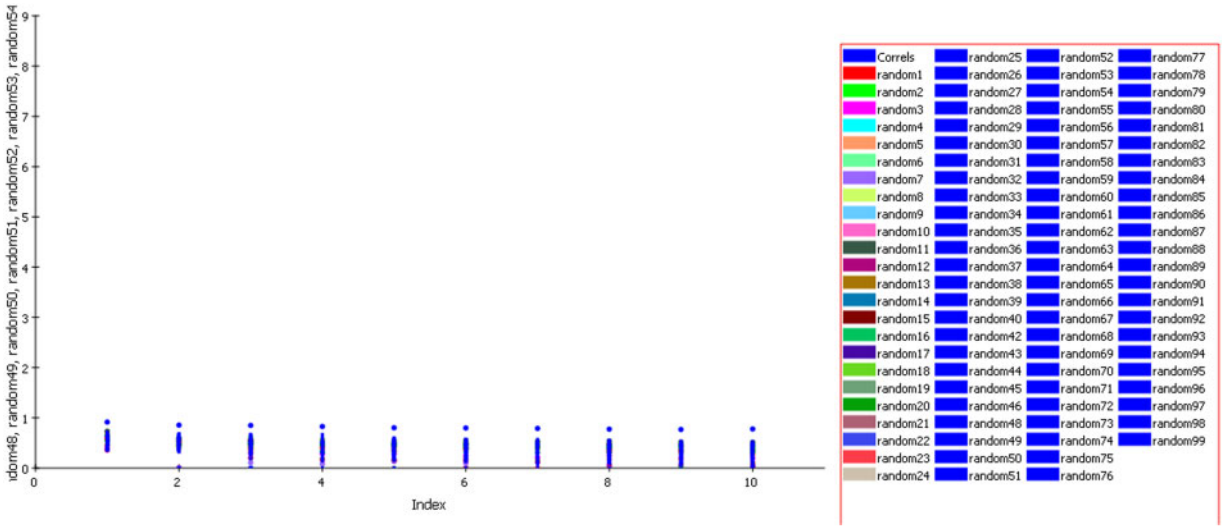

Figure 3: Graph of 99% cat-scrambled correlation data. None of the outcome hypotheses has a higher correlation score than the initial (best) hypothesis.

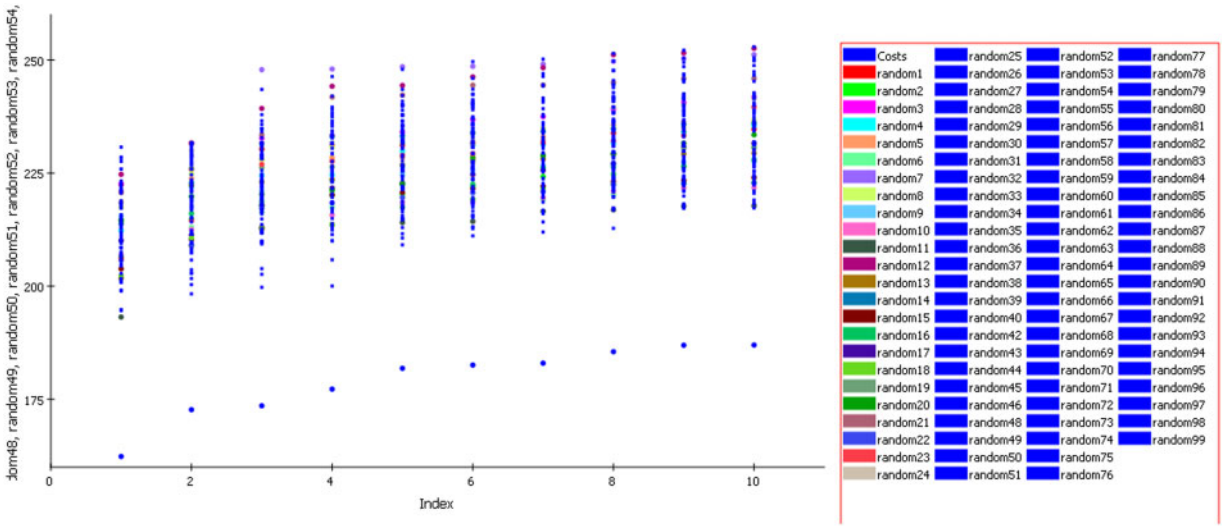

Figure 4: Graph of 99% cat-scrambled cost data. None of the outcome hypotheses has a higher correlation score than the initial (best) hypothesis.

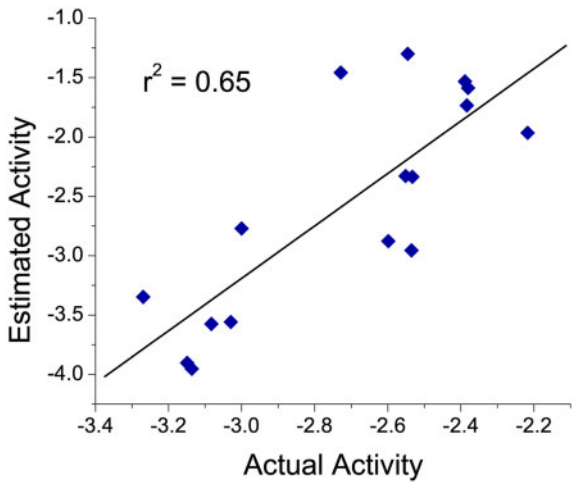

Figure 5: A plot of actual versus estimated biological activity for test set compounds.

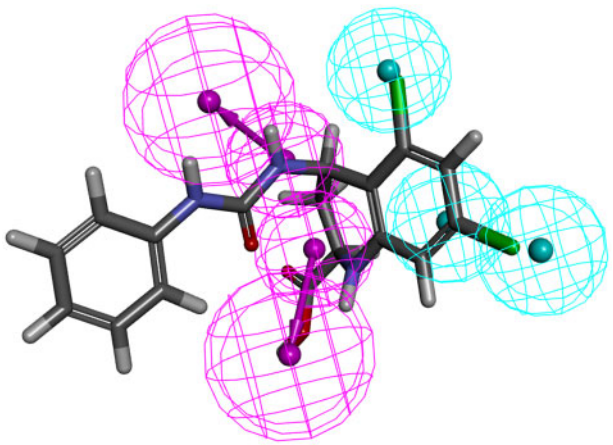

Figure 6: Pharmacophore mapping of most active compound of an external test set onto the chosen pharmacophore model (Hypo1).

methoxyphenyl amino group is interacting with Tyr214 with an interfeature distance of 1.031. The interaction analysis of memantine shows hydrogen bond interactions with amino acid residues His88, Tyr214, and Gly13 (Fig. 8B). Considering the fit values, estimated activity, drug-likeness, docking score, and availability for procuring, HTS 00987 is checked for novelty by employing pairwise Tanimoto similarity indices using "Find Similar Molecules by Fingerprint" in DS. HTS 00987 shows low Tanimoto similarity indices of 0.014 to all the structures of known NMDAR inhibitors proving their novelty. Hence, during this research attempt, we discover one druggable potent N-methyl-D-aspartate receptor antagonist, which can be further explored in clinical trials.

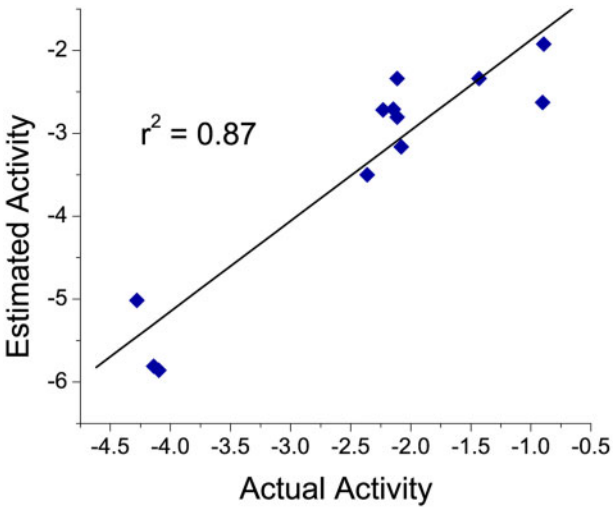

Figure 7: A plot of actual versus estimated biological activity for external test set compounds.

Table 3: A list of the top 10 virtual hits with their ranking values in terms of fit value, estimated value, and LibDock score

S. No.	Maybridge	Fit value	Estimated value	LibDock score
1	HTS 00987	10.18	0.01	114.714
2	RJC 02639	9.64	0.05	112.358
3	SEW 03147	9.53	0.06	110.186
4	HTS 05292	9.33	0.1	109.006
5	RJC 01732	9.15	0.11	99.425
6	BTB 06769	9.05	0.12	98.869
7	BTB 14180	9	0.38	96.52
8	AW 00785	8.64	0.39	96.009
9	JFD 02217	8.37	0.44	95.103
10	BTB 13600	8.19	1.56	95.214

Analysis of the *in vivo* studies

After rigorous validation, HTS 00987 is subjected to *in vivo* studies. The experimental study is framed in a way that the impact of all the standard and test drugs can be assessed after 7 and 14 days against diazepam-induced amnesia. The cognitive parameters are evaluated 30 min after the administration of inducing agent (diazepam) using an eight-arm radial maze as shown in Fig. 9. On Days 7 and 14, the lead compound (HTS 00987) demonstrates a significant increase in number of entries and duration in baited arms (Day 7: $M = 17.25$, $SD = 1.5$; Day 14: $M = 21.5$, $SD = 2.3$, $P < 0.05$) as compared to memantine (Day 7: $M = 14.75$, $SD = 2.38$; Day 14: $M = 16.85$, $SD = 2.21$) as shown in Fig. 10A. Similarly, we observe an increase in duration in baited arms (Day 7: $M = 364.37$, $SD = 5$; Day 14: $M = 386.72$, $SD = 4.1$, $P < 0.05$) when compared to memantine (Day 7: $M = 234.45$, $SD = 4.01$; Day 14: $M = 369.19$, $SD = 5$, $P < 0.05$) (Fig. 10B). The results also show a significant decrease in RME (Day 7: $M = 15.75$, $SD = 3.61$; Day 14: $M = 7.25$, $SD = 1.88$, $P < 0.05$), and WME (Day 7: $M = 4$, $SD = 0.62$; Day 14: $M = 3.5$, $SD = 0.86$, $P < 0.05$) when compared with memantine [RME (Day 7: $M = 16$, $SD = 5.23$; Day 14: $M = 13.25$, $SD = 4.12$), WME (Day 7: $M = 6$, $SD = 1.12$; Day 14: $M = 5.25$, $SD = 2.93$)] which is clearly seen in Fig. 10C. Another major cognitive parameter, percent choice is also calculated and it is observed that HTS 00987 demonstrates a high percent choice (Day 7: $M = 54.14$, $SD = 1.05$; Day 14: $M = 55.98$, $SD = 2.01$, $P < 0.05$) when compared with memantine (Day 7: $M = 47.5$, $SD = 1.11$; Day 14: $M = 52.5$, $SD = 1.89$, $P < 0.05$) as shown in Fig. 10D.

We also compared the results of the Days 8 and 14 of the treatment group with the control group by using the multivariate analysis of variance statistical test [59]. We observed that

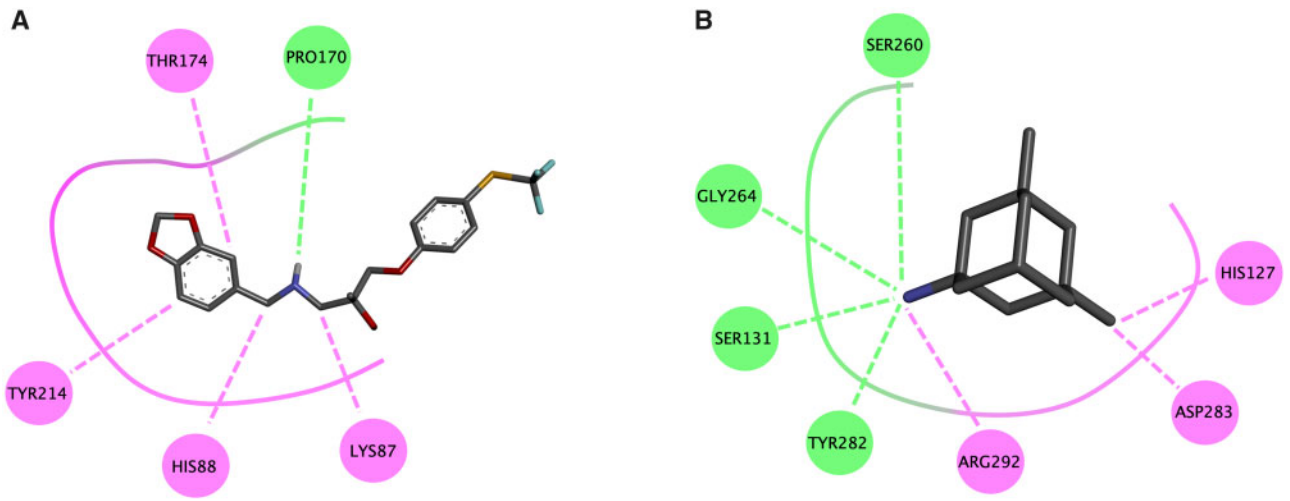

Figure 8: (A) Interaction of HTS 00987 with Tyr214, Thr174, Pro170, His88, and Lys87 in the active site (Green dotted lines represent hydrogen bond interactions; pink dotted lines represent Van der Waals interaction). (B) Interaction of memantine with Ser131, Tyr282, Gly264, Ser260, Asp283, His127, and Arg292 in the active site (green dotted lines representing hydrogen bond interactions; pink dotted lines representing Van der Waals interaction).

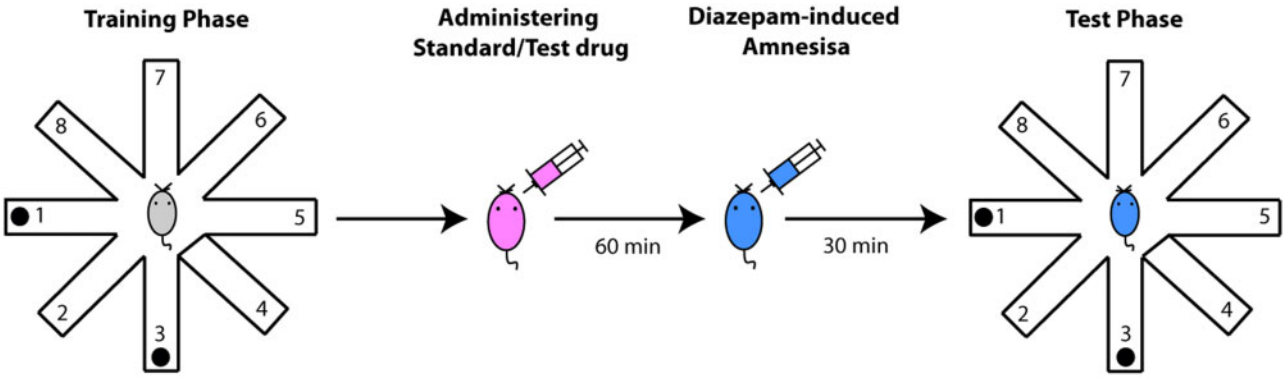

Figure 9: The schematic diagram of the eight-arm radial maze. The animals were tested in the RAM 30 min after the administration of inducing agent (diazepam).

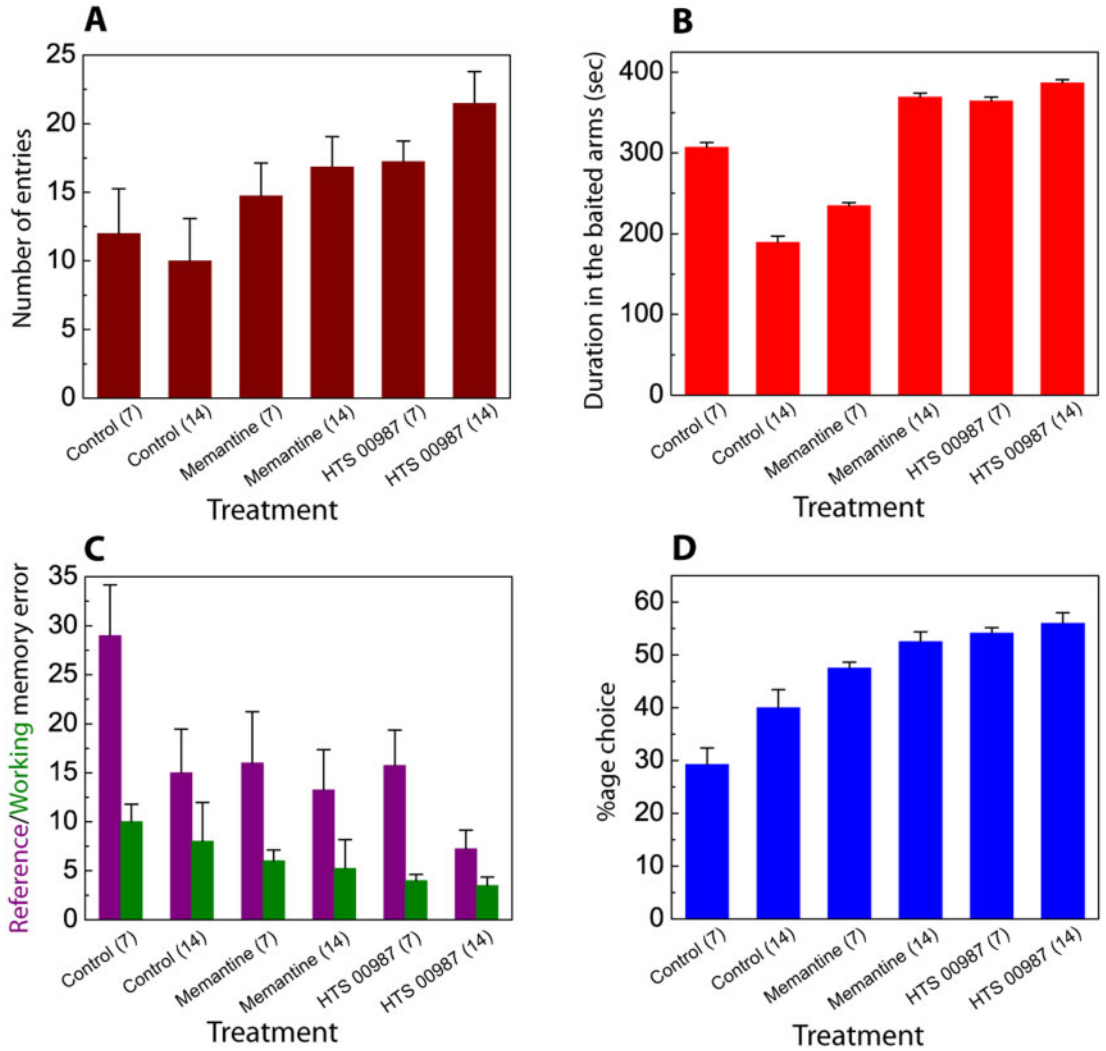

Figure 10: The effects of control (CMC), standard (memantine), and test (HTS 00987) on an eight-arm radial maze in diazepam-induced amnesia in mice: (A) Number of entries in the baited arm. (B) Duration in baited arms (in seconds). (C) Reference/WMEs. (D) Percentage of correct choices. The error bars correspond to the SD of the measurements.

important parameters such as the number of entries, duration in the baited arm, WME, RME, and percent choice showed significant *P*-values, consequently, validating our experimental results. The *P*-values for the parameters are presented in the supplementary information (Supplementary Table S1). In summary, HTS 00987 shows a remarkable increase in the number of entries in the baited arm, duration in baited arms, percent correct choice, and a significant decrease in RME and WME in diazepam-induced amnesia in mice as compared to memantine during Week 1 and surprisingly its repeated administration also

showed a noteworthy increase in memory. In view of the results, it can be concluded that HTS 00987 has shown good neuroprotection properties and the lead compound can be subjected to clinical trials for their development as novel drugs.

Conclusion

In this study, we have used a four-phase approach to identify druggable compounds to treat AD. A thoroughly validated pharmacophore model was used for the identification of lead compounds for treating AD. Of the shortlisted leads, HTS 00987, exhibited good *in vivo* potency, which is evident by a higher percent choice and duration of mice staying in the baited arm. Our attempt to compare the test drug (HTS 00987) with memantine (a well-known drug for treating AD) gives us confidence that HTS 00987 is another emerging, equally effective therapy for treating AD. This preliminary result lays a solid foundation for carrying out further experimental studies to find a novel drug candidate to treat AD. Furthermore, the identified compounds can also serve as a template for designing new NMDA receptor antagonists. Therefore, we propose that ligand-based pharmacophore modeling coupled with experiments can prove to be an adequate reservoir for identifying novel leads/hits from the chemical compound databases.

Supplementary data

Supplementary data is available at *Biology Methods and Protocols* online.

Ethics approval and consent to participate

Ethics approval and consent to participate are not available, as this study does not involve any clinical studies.

Conflict of interest statement

The authors declare that they have no competing interests.

Authors' contributions

M.S. performed the whole experiments. S.P. conceptualized and designed the project. S.S. made substantial contributions to the pharmacological studies. A.M. and A.S. supported in analyzing the results. M.S. wrote the manuscript. A.K.J. helped in critical editing of the manuscript. All authors read and approved the final manuscript.

Data availability statements

The datasets used/produced during and/or evaluated throughout this study are obtainable from the corresponding author on request.

References

1. Salituro FG, Harrison BL, Baron BM *et al.* 3-(2-Carboxyindol-3-yl) propionic acid-based antagonists of the NMDA (N-methyl-D-aspartic acid) receptor associated glycine binding site. *J Med Chem* 1992;**35**:1791–9.
2. Hansen KB, Yi F, Perszyk RE *et al.* NMDA receptors in the central nervous system. *Methods Mol Biol* 2017;**1677**:1–80.
3. Cull-Candy S, Brickley S, Farrant M. NMDA receptor subunits: diversity, development and disease. *Curr Opin Neurobiol* 2001; **11**:327–35.
4. Kew JN, Trube G, Kemp JA. State-dependent NMDA receptor antagonism by Ro 8-4304, a novel NR2B selective, non-competitive, voltage-independent antagonist. *Br J Pharmacol* 1998;**123**:463–72.
5. Chenard BL, Menniti FS. Antagonists selective for NMDA receptors containing the NR2B subunit. *Curr Pharm Des* 1999; **5**:381–404.
6. Papouin T, Ladépêche L, Ruel J *et al.* Synaptic and extrasynaptic NMDA receptors are gated by different endogenous coagonists. *Cell* 2012;**150**:633–46.
7. Tanqueiro SR, Ramalho RM, Rodrigues TM *et al.* Inhibition of NMDA receptors prevents the loss of BDNF function induced by amyloid *β*. *Front Pharmacol* 2018;**9**:237.
8. Hardingham GE. Targeting synaptic NMDA receptor co-agonism as a therapy for Alzheimer's disease? *Cell Metab* 2020;**31**:439–40.
9. Bobich JA, Zheng Q, Campbell A. Incubation of nerve endings with a physiological concentration of A*β*1-42 activates CaV2.2(N-Type)-voltage operated calcium channels and acutely increases glutamate and noradrenaline release. *J Alzheimers Dis* 2004;**6**:243–55.
10. Keana JF, McBurney RN, Scherz MW *et al.* Synthesis and characterization of a series of diarylguanidines that are noncompetitive N-methyl-D-aspartate receptor antagonists with neuroprotective properties. *Proc Natl Acad Sci USA* 1989;**86**:5631–5.
11. Blanco-Silvente L, Capellà D, Garre-Olmo J *et al.* Predictors of discontinuation, efficacy, and safety of memantine treatment for Alzheimer's disease: meta-analysis and meta-regression of 18 randomized clinical trials involving 5004 patients. *BMC Geriatr* 2018;**18**:168.
12. Sharma M, Jainarayanan AK. AchE-OGT dual inhibitors: potential partners in handling Alzheimer's disease. 2018, 10.1101/303040.
13. Gunner OA. *Pharmacophore, Perception, Development, and Use in Drug Design*. San Diego: University International Line, 2007, 17–20.
14. Singh A, Paliwal S, Sharma M *et al.* Identification of novel antifungal lead compounds through pharmacophore modeling, virtual screening, molecular docking, antimicrobial evaluation, and gastrointestinal permeation studies. *J Biomol Struct Dynam* 2017;**35**:2363–71.
15. Li H, Sutter J, Hoffman R. HypoGen: an automated system for generating 3D predictive pharmacophore models. In: *Pharmacophore Perception, Development, and Use in Drug Design*. La Jolla, CA: International University Line, 1999, 171–89.
16. Reddy NL, Hu L-Y, Cotter RE *et al.* Synthesis and structure-activity studies of N, N'-diarylguanidine derivatives. N-(1-naphthyl)-N'-(3-ethylphenyl)-N'-methylguanidine: a new, selective noncompetitive NMDA receptor antagonist. *J Med Chem* 1994;**37**:260–7.
17. Kurogi Y, Guner O. Pharmacophore modeling and three-dimensional database searching for drug design using catalyst. *Curr Med Chem* 2001;**8**:1035–55.
18. Meganathan C, Sakkiah S, Lee Y *et al.* Discovery of potent inhibitors for interleukin-2-inducible T-cell kinase: structure-based virtual screening and molecular dynamics simulation approaches. *J Mol Model* 2013;**19**:715–26.
19. Tripathi N, Paliwal S, Sharma S *et al.* Discovery of novel soluble epoxide hydrolase inhibitors as potent vasodilators. *Sci Rep* 2018;**8**:14604.
20. Guner O. History and evolution of the pharmacophore concept in computer-aided drug design. *Curr Top Med Chem* 2002;**2**:1321–32.
21. Debnath AK. Pharmacophore mapping of a series of 2,4-diamino-5-deazapteridine inhibitors of mycobacterium avium complex dihydrofolate reductase. *J Med Chem* 2002;**45**:41–53.

22. Pal S, Kumar V, Kundu B *et al.* Ligand-based pharmacophore modeling, virtual screening and molecular docking studies for discovery of potential topoisomerase I inhibitors. *Comput Struct Biotechnol J* 2019;**17**:291–310.
23. Pal M, Paliwal S. In silico identification of novel lead compounds with AT1 receptor antagonist activity: successful application of chemical database screening protocol. *Org Med Chem Lett* 2012;**2**:7.
24. Sakkiah S, Thangapandian S, John S *et al.* 3D QSAR pharmacophore based virtual screening and molecular docking for identification of potential HSP90 inhibitors. *Eur J Med Chem* 2010;**45**:2132–40.
25. Singh A, Paliwal SK, Sharma M *et al.* In silico and in vitro screening to identify structurally diverse non-azole CYP51 inhibitors as potent antifungal agent. *J Mol Graph Model* 2016;**63**:1–7.
26. Lipton SA. Paradigm shift in neuroprotection by NMDA receptor blockade: memantine and beyond. *Nat Rev Drug Discov* 2006;**5**:160–70.
27. Mittal A, Paliwal S, Sharma M *et al.* Pharmacophore based virtual screening, molecular docking and biological evaluation to identify novel PDE5 inhibitors with vasodilatory activity. *Bioorg Med Chem Lett* 2014;**24**:3137–41.
28. Acharya BN, Kaushik MP. Pharmacophore-based predictive model generation for potent antimalarials targeting haem detoxification pathway. *Med Chem Res* 2007;**16**:213–29.
29. Bhattacharjee A, Mylliemngap BJ, Velmurugan D. 3D-QSAR studies on fluroquinolones derivatives as inhibitors for tuberculosis. *Bioinformation* 2012;**8**:381–7.
30. Mehta H, Khokra SL, Arora K *et al.* Pharmacophore mapping and 3D-QSAR analysis of Staphylococcus Aureus Sortase a inhibitor. *Der Pharma Chemica* 2012;**4**:1776–84.
31. Chandra KU, Haripriya M, Shaik M. 2D QSAR, pharmacophore and docking studies of mycobacterium tuberculosis enoyl acyl carrier protein reductase inhibitors. *J Global Pharma Technol* 2010;**2**:73–89.
32. Walters W, Stahl MT, Murcko MA. Virtual screening—an overview. *Drug Discov Today* 1998;**3**:160–78.
33. Yadav D, Paliwal S, Yadav R *et al.* Identification of novel HIV 1-protease inhibitors: application of ligand and structure based pharmacophore mapping and virtual screening. *PLoS ONE* 2012;**7**:e48942.
34. Hou T, Xu X. Recent development and application of virtual screening in drug discovery: an overview. *Curr Pharm Des* 2004;**10**:1011–33.
35. Anderson A, Wright D. The design and docking of virtual compound libraries to structures of drug targets. *Curr Comput Aid Drug* 2005;**1**:103–27.
36. Misra S, Saini M, Ojha H *et al.* Pharmacophore modelling, atom-based 3D-QSAR generation and virtual screening of molecules projected for mPGES-1 inhibitory activity. *SAR QSAR Environ Res* 2017;**28**:17–39.
37. Daisy P, Suveena S, Lilly V. Molecular docking of medicinal compound Lupeol with autolysin and potential drug target of UTI. *J Chem Pharm Res* 2011;**3**:557–62.
38. Peng J, Li Y, Zhou Y *et al.* Pharmacophore modeling, molecular docking and molecular dynamics studies on natural products database to discover novel skeleton as non-purine xanthine oxidase inhibitors. *J Recept Sig Transd* 2018;**38**:246–55.
39. Paliwal S, Mittal A, Sharma M *et al.* Pharmacophore and molecular docking based identification of novel structurally diverse PDE-5 inhibitors. *Med Chem Res* 2015;**24**:576–87.
40. Sharma M, Mittal A, Singh A *et al.* Identification of novel and structurally diverse N-methyl-D-aspartate receptor antagonists: successful application of pharmacophore modeling, virtual screening and molecular docking. 2018, 10.1101/314914
41. Wu F, Xu T, He G *et al.* Discovery of novel focal adhesion kinase inhibitors using a hybrid protocol of virtual screening approach based on multicomplex-based pharmacophore and molecular docking. *Int J Mol Sci* 2012;**13**:15668–78.
42. Meng X, Zhang H, Mezei M *et al.* Molecular docking: a powerful approach for structure-based drug discovery. *Curr Comput Aided Drug Des*2011;**7**:146–57.
43. Liu P, Bilkey DK. The effect of excitotoxic lesions centered on the perirhinal cortex in two versions of the radial arm maze task. *Behav Neurosci* 1999;**113**:672–82.
44. Suzuki S, Augerinos G, Black AH. Stimulus control of spatial behavior on the eight-arm maze in rats. *Learn Motiv* 1980;**11**:1–18.
45. Kulkarni K, Kasture S, Mengi S. Efficacy study of prunus amygdalus (almond) nuts in scopolamine-induced amnesia in rats. *Indian J Pharmacol* 2010;**42**:168.
46. Prabhakar S, Saraf MK, Pandhi P *et al.* Bacopa monniera exerts antiamnesic effect on diazepam-induced anterograde amnesia in mice. *Psychopharmacology* 2008;**200**:27–37.
47. Olthof A, Sutton JE, Slumskie SV *et al.* In search of the cognitive map: can rats learn an abstract pattern of rewarded arms on the radial maze? *J Exp Psychol Anim Behav Process* 1999;**25**:352–62.
48. O'Keefe J, Nadel L. *The Hippocampus as a Cognitive Map*. Oxford: Oxford University Press, 1978
49. Rao N, Chou T, Ventura D *et al.* Investigation of the pharmacokinetic and pharmacodynamic interactions between memantine and glyburide/metformin in healthy young subjects: a single-center, multiple-dose, open-label study. *Clin Ther* 2005; **27**:1596–606.
50. Joo IS, Hwang DH, Seok JI *et al.* Oral administration of memantine prolongs survival in a transgenic mouse model of amyotrophic lateral sclerosis. *J Clin Neurol* 2007;**3**:181–6.
51. Tampi RR, van Dyck CH. Memantine: efficacy and safety in mild-to-severe Alzheimer's disease. *Neuropsychiatr Dis Treat* 2007;**3**:245–58.
52. Brown MF, Wintersteen J. Spatial patterns and memory for locations. *Anim Learn Behav* 2004;**32**:391–400.
53. Gökçek-Saraç Ç, Wesierska M, Jakubowska-Doğru E. Comparison of spatial learning in the partially baited radial-arm maze task between commonly used rat strains: wistar, Sprague-Dawley, Long-Evans, and outcrossed Wistar/Sprague-Dawley. *Learn Behav* 2015;**43**:83–94.
54. Kay C, Harper D, Hunt M. Differential effects of MDMA and scopolamine on working versus reference memory in the radial arm maze task. *Neurobiol Learn Memory* 2010;**93**:151–6.
55. Kim H, Park JY, Kim KK. Spatial learning and memory using a radial arm maze with a head-mounted display. *Psychiatry Investig* 2018;**15**:935–44.
56. Gawel K, Gibula E, Marszalek-Grabska M *et al.* Assessment of spatial learning and memory in the Barnes maze task in rodents-methodological consideration. *Naunyn-Schmiedeberg's Arch Pharmacol* 2019;**392**:1–18.
57. Castner S, Goldman-Rakic P, Williams G. Animal models of working memory: insights for targeting cognitive dysfunction in schizophrenia. *Psychopharmacology* 2004;**174**:111–25.
58. John S, Thangapandian S, Sakkiah S *et al.* Potent bace-1 inhibitor design using pharmacophore modeling, in silico screening and molecular docking studies. *BMC Bioinformatics* 2011;**12**:S28.
59. Clavel J, Morlon H. Reliable phylogenetic regressions for multivariate comparative data: illustration with the MANOVA and application to the effect of diet on mandible morphology in Phyllostomid bats. *Syst Biol* 2020, 10.1093/sysbio/syaa010.